



# Integrating a global glacier model into local hydrological modeling: Impacts on melt contributions

Justine Berg<sup>1</sup>, Pascal Horton<sup>1</sup>, Martina Kauzlaric<sup>1</sup>, Alexandra von der Esch<sup>2,3</sup>, and Bettina Schaeffli<sup>1</sup>

<sup>1</sup>Institute of Geography (GIUB) and Oeschger Centre for Climate Change Research (OCCR), University of Bern, Hallerstrasse 12, Bern 3012, Switzerland

<sup>2</sup>Laboratory of Hydraulics, Hydrology and Glaciology (VAW), ETH Zurich, Zurich, Switzerland

<sup>3</sup>Swiss Federal Institute for Forest, Snow and Landscape Research (WSL), bâtiment ALPOLE, Sion, Switzerland

**Correspondence:** Justine Berg (justine.berg@unibe.ch)

**Abstract.** Snow and glacier meltwater are critical water resources for mountain regions, yet their accurate representation in hydrological models remains challenging. As climate change alters the timing and magnitude of melt contributions, accurate partitioning between snow and glacier sources becomes increasingly important. To address this challenge, this study couples the hydrological model HBV (as implemented in the Raven modeling framework) with the Global Glacier Evolution Model  
5 GloGEM and integrates a snow redistribution scheme for application across 14 glaciated headwater catchments in Switzerland. At this local catchment scale, we investigate whether glacier constraints and the addition of snow redistribution reduce parameter equifinality and increase the reliability of melt contribution estimates. Simulations are evaluated against observed streamflow, gridded snow water equivalent data, and glacier melt data based on observed mass balance. The gravitational snow redistribution algorithm successfully prevents unrealistic high-elevation snow accumulation and improves catchment average  
10 SWE simulation performance. Uncoupled HBV configurations outperform coupled HBV-GloGEM setups according to streamflow metrics. However, this superior performance is achieved by simulating glacier melt rates exceeding GloGEM estimates and glacier storage change data by factors of 2-3 in some catchments, effectively using glacier ice to offset precipitation biases in forcing data, which can be critical for climate change impact studies. Glacier melt contributions can vary by nearly an order of magnitude among best-performing parameter sets, highlighting severe parameter equifinality. Coupling with GloGEM,  
15 calibrated using glacier-specific geodetic mass balance, produces glacier melt consistent with observations and substantially improves identifiability of both glacier and snowmelt contributions. Despite lower streamflow performance metrics, glacier melt constraints prevent compensatory errors that would compromise projections as melt dynamics shift under climate change. Applying this framework to future climate scenarios and integrating additional constraints such as snow observations may further improve the reliability of melt contribution projections.

## 20 1 Introduction

Many mountainous and high-latitude regions around the globe receive the majority of their annual precipitation as snow and rely on snow and glacier meltwater for agriculture and human consumption (Kaser et al., 2010; Mankin et al., 2015; Huss and Hock, 2018; Viviroli et al., 2020). This highlights the importance of the cryosphere as temporary water storage, reducing

interannual streamflow variability by accumulating precipitation during cold and wet seasons and releasing it during warm  
25 and dry periods (Jansson et al., 2003; Viviroli et al., 2011). This delayed release helps mitigate extreme water shortages on  
seasonal and longer time scales, sustaining downstream water supply for regional ecosystems, groundwater recharge, human  
consumption, irrigation, and hydropower (Freudiger et al., 2017; Biemans et al., 2019; van Tiel et al., 2020). It is therefore  
essential to understand the impact of climate change on the cryosphere and river streamflow for sustainable water management  
of future water resources (Molden et al., 2017).

30 Rising global temperatures are expected to reduce the water storage capacity of both glaciers and snowpack, which will have  
major consequences for the downstream water supply (Immerzeel et al., 2020). As both the fraction and frequency of snowfall  
are declining (Frei et al., 2018), the extent of snow-covered areas in the Alps is decreasing (Sturm et al., 2017; Hanzer et al.,  
2018). Consequently, the snow cover season in mountain regions is projected to shorten, with a delayed onset of snow cover  
and an earlier onset of snow melting, leading to a shift of the peak melting season towards earlier periods (Arnoux et al., 2021).  
35 Most glaciers have lost and continue to lose a substantial part of their volume and area (Hugonnet et al., 2021). Farinotti et al.  
(2012) found a combined response to this glacier loss with first increasing and then decreasing annual streamflow depending  
on the glacier volume in the catchment, illustrating the 'peak water' effect. As a result, snow- and ice-dominated catchments  
are expected to experience altered flow seasonality, with higher winter discharge and reduced summer runoff (Horton et al.,  
2006; Han et al., 2024), affecting water availability in downstream regions (Arnoux et al., 2021).

40 To predict these hydrological changes, it is essential to include an accurate representation of glacier and snowpack projec-  
tions in hydrological models. A range of modeling approaches with varying complexity have been developed and applied in  
snow- and ice-dominated mountainous catchments (e.g., Hock, 2003; Hanzer et al., 2018; Immerzeel et al., 2020). Hydro-  
logical models often rely on temperature-index approaches to simulate snow accumulation and melt while neglecting snow  
redistribution processes. This can produce unrealistic snow accumulation patterns with excessive snow storage at high eleva-  
45 tions known as 'snow towers' (Freudiger et al., 2017). In reality, post-depositional processes such as wind-driven transport  
(Winstral et al., 2017; Reynolds et al., 2021) and avalanching (Bernhardt and Schulz, 2010) frequently remove snow from  
exposed areas, leaving summits, cliffs, and steep slopes largely snow-free (Freudiger et al., 2017). Ignoring these processes  
can therefore lead to local overestimation of snow water equivalent (SWE). Representing snow redistribution is thus essential  
for accurately simulating catchment-scale SWE and melt dynamics.

50 While incorporating snow redistribution improves the representation of snow processes, another important step toward more  
realistic hydrological modeling in high-elevation regions involves improving glacier dynamics. To this end, a few recent studies  
have coupled large-scale hydrological models with global glacier models (Wiersma et al., 2022; Hanus et al., 2024). Wiersma  
et al. (2022) found that coupling a global hydrological model with a global glacier model increases the performance to re-  
produce basin streamflow in highly glaciated catchments and prevents underestimation of glacier runoff. Hanus et al. (2024)  
55 found that improved glacier representation can prevent underestimations of future streamflow changes, even far downstream at  
the outlet of large glaciated river basins. Although these studies demonstrate the advantages of coupling hydrological models  
with global glacier models, such approaches have been developed primarily for large-scale basins with limited evaluation at  
the local catchment-scale (up to a few hundred km<sup>2</sup>). It remains unclear whether global glacier models provide comparable



benefits when applied at these scales, particularly since small catchments may exhibit different sensitivities to glacier representation than large basins. In one of the few local-scale studies, Pesci et al. (2023) coupled the physically-based hydrological model WaSIM (Schulla and Jasper, 2001) with the Open Global Glacier Model (OGGM) (Maussion et al., 2019) in an Austrian headwater catchment and compared this approach to traditional volume-area scaling (Bahr et al., 1997) to simulate glacier evolution. Although both approaches produced similar results for streamflow during the historical period, they revealed substantial divergences in future projections, suggesting that the choice of glacier representation may have a limited impact on model performance during calibration but significant implications for long-term predictions.

Hydrological modeling remains an essential tool for understanding the hydrological behavior of glaciated catchments and projecting their response to climate change. However, these models often exhibit equifinality, where multiple parameter sets yield similarly good streamflow simulations, but represent underlying processes differently (Beven, 2006). For instance, Stahl et al. (2008) found that equally well-performing streamflow simulations corresponded to widely varying glacier mass balance estimates. This highlights that deficiencies in model input, structure, or parameterization can be compensated (Duethmann et al., 2015). Introducing process-based constraints through glacier model coupling, along with improved snow redistribution schemes, has the potential to reduce such ambiguities. Yet, how these additional constraints affect hydrological model calibration, parameter identifiability, and the quantification of seasonal snow and glacier melt contributions remains largely unexplored. Addressing these questions is key to improving confidence in model-based assessments of future water availability in mountain regions.

To address these challenges, this study applies a modeling framework to 14 glaciated headwater catchments in Switzerland. The framework combines the hydrological modeling framework Raven (Craig et al., 2020) with the global glacier model GloGEM (Huss and Hock, 2015) and integrates a snow redistribution scheme (Bernhardt and Schulz, 2010) to better represent cryospheric dynamics. The simulation results are evaluated against observed streamflow, a gridded SWE product (Marty et al., 2025), and annual glacier storage change data from Switzerland (van Tiel et al., 2025). Finally, we analyze how different model configurations influence calibrated parameter values and assess the resulting impacts on annual and seasonal snow and glacier melt contributions.

## 2 Study site

For this study, 14 glaciated catchments located in the Swiss Alps were selected (Figure 1 & Table 1). This dataset corresponds to all Swiss gauged catchments with glacier cover but largely unaffected by hydropower infrastructure. Dominant land uses in these areas are alpine pastures, natural grasslands, forests, shrubs, water bodies, including lakes, glaciers, rock outcrops and rock debris from periglacial and paraglacial processes (Marsoner et al., 2023). The dominant geology in the catchments is granite and gneiss (Swisstopo - Swiss Federal Office of Topography, 2020). The selected catchments are mesoscale, with areas up to 555 km<sup>2</sup>. They are located at high elevations, with mean catchment elevations ranging from 1811 m asl to 2929 m asl (Table 1). Due to large elevation differences within individual catchments, strong vertical temperature and precipitation gradients are present. Their climate is characterized by low annual average temperatures ranging from -2.8 °C to 3.3 °C and a high



mean annual precipitation ranging between 1149 mm yr<sup>-1</sup> and 1993 mm yr<sup>-1</sup> with a high fraction of precipitation falling as snow, ranging from 26 % in the Kander catchment (ID 2469) and 81 % in the Massa catchment (ID 2161). The Rosegbach catchment (ID 2256) is notably drier than the others since it is located more intra-Alpine. Snow typically covers much of the landscape between November and April, with snowfall possible year-round at higher elevations. The hydrological regimes of the catchments are either glacier-dominated or nival (snowmelt-driven), with peak streamflow occurring during the summer months due to snow and glacier melt (HADES, 2025). Glacier cover in the year 2000 varies substantially between catchments, ranging from 3.2 % in the Rein da Sumvitg catchment (ID 2430) to 60.1 % in the Massa catchment (ID 2161), according to the RGI v6.0 glacier outlines (RGI Consortium, 2017).

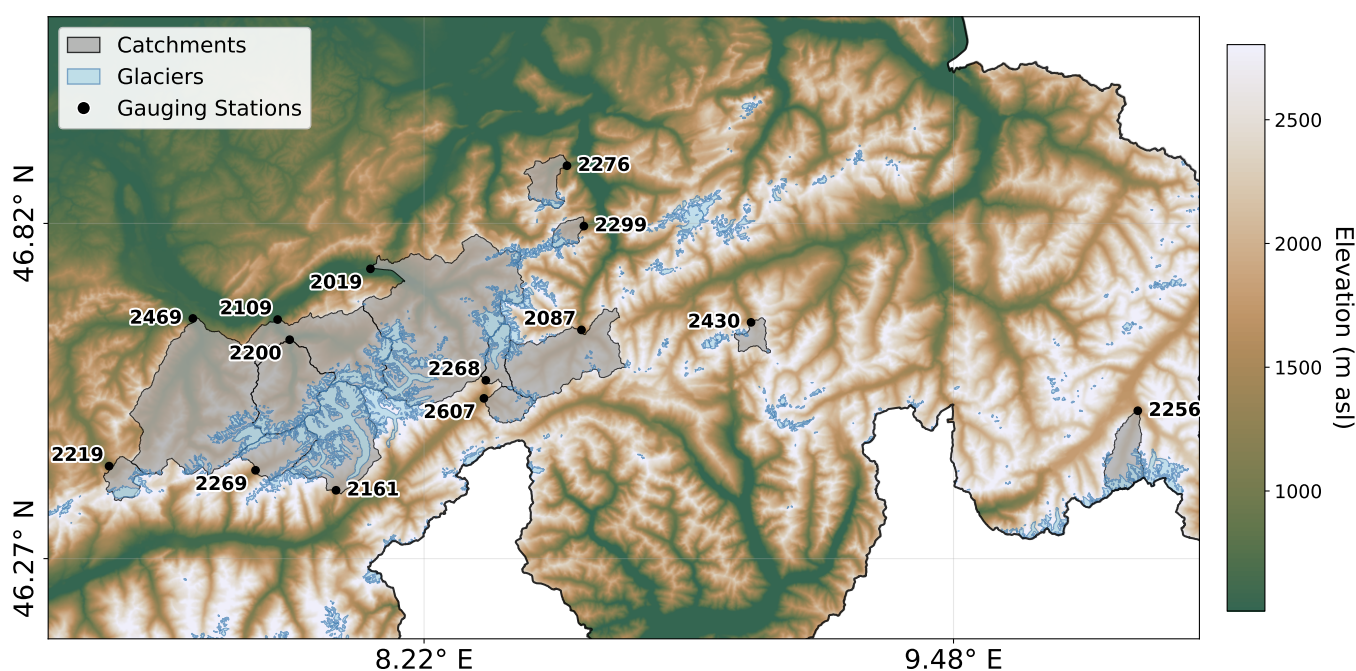


**Figure 1.** Map of study area in Switzerland with SwissTopo DEM (Swisstopo - Swiss Federal Office of Topography, 2020). Grey polygons show selected catchments with their CAMELS-CH ID and gauging station (black point), and light blue polygons the glaciated area according to RGI v6.0 with the reference year 2000.

### 100 3 Methodology

An automated workflow was developed to set up the hydrological model for all catchments of interest in Switzerland. The required input datasets and model components are described in Sections 3.1 and 3.2. The workflow automatically generates inputs for the hydrological model, calibrates the model, and runs simulations for each catchment, as described in Sections 3.3 to 3.5.



**Table 1.** Overview of the selected catchments. Reference period for mean annual temperature, precipitation and streamflow: 2000 - 2021 (MeteoSwiss, 2013). Reference year for relative glacier area: 2000 (RGI Consortium, 2017).

CAMELS-CH ID	gauging station	river	area (km <sup>2</sup> )	mean elevation (m asl)	glacier area (%)	mean annual precipitation (mm yr <sup>-1</sup> )	mean annual streamflow (mm yr <sup>-1</sup> )	mean temperature (°C)
2019	Brienziwiler	Aare	555.2	2127	17.5	1828	2074	1.4
2087	Andermatt	Reuss	190.2	2276	3.4	1676	1167	0.5
2109	Gsteig	Lütschine	380.7	2039	15.9	1801	1572	2.2
2161	Blatten b. Naters	Massa	195.5	2929	60.1	1993	2527	-2.8
2200	Zweilütschine	Weisse Lütschine	164.9	2148	16.0	1808	1500	1.2
2219	Oberried / Lenk	Simme	34.7	2331	25.3	1747	2168	0.9
2256	Pontresina	Rosegbach	66.5	2700	25.5	1149	1369	-1.8
2268	Gletsch	Rhone	39.4	2701	44.1	1887	2314	-1.8
2269	Blatten	Lonza	77.4	2615	28.5	1603	1917	-1.8
2276	Isenthal	Grosstalbach	43.9	1811	7.1	1747	1305	3.1
2299	Erstfeld-Bodenberg	Alpbach	20.7	2186	22.1	1651	2352	0.8
2430	Sumvitg-Encardens	Rein da Sumvitg	21.8	2445	3.2	1571	2213	-0.2
2469	Hondrich	Kander	490.7	1846	6.1	1475	1379	3.3
2607	Oberwald	Goneri	38.6	2372	5.3	1931	1959	0.0

### 105 3.1 Data

CAMELS-CH (Catchment Attributes and Meteorology for Large-sample Studies – Switzerland) is an open large-sample hydro-meteorological dataset including data for 331 stream and lake catchments in Switzerland (Höge et al., 2023). In this study, we use the available daily streamflow time series from 2000 to 2021, along with the corresponding catchment outlines. The meteorological forcing data consist of daily 1 km<sup>2</sup> gridded products from MeteoSwiss, which provide mean (TabsD), minimum (TminD), and maximum (TmaxD) air temperature, as well as daily precipitation totals (RhiresD) (MeteoSwiss, 2013). Catchment characteristics are described using the SwissTopo 25 m digital elevation model (DEM) (Swisstopo - Swiss Federal Office of Topography, 2020), the ESA WorldCover v2 land-use dataset (ESA WorldCover, 2021), and the RGI v6.0 glacier outlines (RGI Consortium, 2017). For the validation of SWE simulations, the SPASS dataset is used (Marty et al., 2025). This dataset provides daily 1 km gridded SWE over Switzerland, generated using a temperature-index model operated by the Operational Snow Hydrological Service (OSHD). To improve simulations, the model assimilates in-situ snow depth observations from 350 stations using an Ensemble Kalman Filter (Magnusson et al., 2014). To evaluate the simulated glacier melt, a dataset developed by van Tiel et al. (2025) is used for the annual glacier melt. This dataset consists of annual glacier mass balances for each individual Swiss glacier estimated by extrapolating mass balance anomalies from 28 surveyed glaciers using inverse-distance



weighting and then combining these with geodetic mass balances derived from digital elevation models to constrain long-term  
120 mass changes.

## 3.2 Models

This study couples the Global Glacier Evolution Model (GloGEM) (Huss and Hock, 2015) with the flexible hydrological modeling framework Raven (Craig et al., 2020) to simulate the combined effects of glacier evolution and catchment hydrology on streamflow. The following subsections provide a brief description of each model and its relevant configurations.

### 125 3.2.1 Glacier model

GloGEM is designed to simulate glacier mass balance and related geometric changes for individual glaciers worldwide (Huss and Hock, 2015). A detailed description of the model can be found in Huss and Hock (2015). The model can be applied to a single glacier, to multiple glaciers within a catchment, to all glaciers within a given Randolph Glacier Inventory (RGI) region, or globally by running the model for all RGI regions. The model calculates all major components of the glacier mass budget  
130 (snow accumulation, snowmelt, ice melt, and refreezing) distributed over 10 m elevation bands for each glacier, at a monthly or daily temporal resolution. In this study, we use the daily resolution in order to resolve short-term variations in the input forcing as well as daily runoff dynamics from glacier and snow melt.

The mass balance is estimated with a temperature-index model (Hock, 2003), which links positive air temperatures to melt through degree-day factors. Distinct degree-day factors are applied for snow and ice, with the snow factor being calibrated and  
135 the ice factor set to twice the snow factor ( $f_{ice} = 2f_{snow}$ ) to account for different melt rates (Hock, 2003). Glacier geometry is held constant up to the year 2000, corresponding to the date of the RGI v6.0 outlines, after which it evolves annually based on modeled mass changes. Glacier dynamics are simulated using an empirical relationship that connects thickness change to the normalized elevation range, enabling the modeling of glacier advance/retreat and surface elevation change (dh-parameterization; Huss et al., 2010). Simulated meltwater from snow and ice as well as liquid precipitation, is assumed to  
140 contribute directly to the glacier runoff (Huss and Hock, 2018). For glacier runoff calculations, a constant contributing area is assumed, defined as the RGI v6.0 glacier area within each basin.

### 3.2.2 Hydrological model

Raven is a flexible hydrological modeling framework offering a wide range of modeling options (Craig et al., 2020). It supports discretization from a single lumped watershed to fully distributed models. The land surface can be subdivided into subbasins,  
145 which are further composed of hydrological response units (HRUs). Lateral flow within each subbasin is represented by a non-spatial transfer function that accounts for delay and redistribution before water reaches the subbasin outlet. Further, the model supports flexible process representation ranging from simple empirical models to more complex process-based schemes. This allows the user to adjust their model according to the importance of processes or data availability. This flexibility in process representation allows Raven to emulate several existing hydrological models (e.g. HBV, HYMOD, GR4J).



150 For this study, we emulate the HBV (Hydrologiska Byråns Vattenbalansavdelning) model, a conceptual precipitation-streamflow model (Bergström, 1995). HBV is widely applied in mountainous catchments and includes a simple glacier melt parameterization, making it well-suited for comparing simulated glacier melt between its native glacier module and GloGEM. The HBV glacier model calculates the melt rate based on the potential melt and a glacial melt correction factor applied to the degree day factor of snow ( $f_{MELT\_FACTOR}$ ) (Table 2). No glacier melt occurs if there is any snow cover on the glacier area. The

155 calculated meltwater is then released with a simple linear storage coefficient approach, where the glacier storage coefficient is a calibrated model parameter ( $f_{GLAC\_STORAGE\_COEFF}$ ). The snow routine determines whether precipitation falls as rain or snow according to a temperature threshold ( $f_{RAINSNOW\_TEMP}$ ). Snowmelt is modeled using a modified degree-day method where the melt factor ( $f_{MELT\_FACTOR}$ ) varies seasonally between minimum and maximum values and is adjusted for forest cover and terrain aspect. The model accounts for the refreezing of liquid water during periods below freezing temperature ( $f_{REFREEZE\_FACTOR}$ ).

160 HBV has two conceptual groundwater reservoirs: an upper zone for quick response (interflow) and a lower zone for baseflow. Each is depleted by linear recession equations with different coefficients ( $f_{BASEFLOW\_COEFF}$ ). The transfer function translates HRU outflow into river discharge using a triangular weighting function ( $f_{TIME\_CONC}$ ). For a more detailed description of model components the reader is referred to the Raven User's and Developer's Manual (Craig, 2025). Parameter ranges for the HBV emulation were taken from the RavenPy repository (<https://github.com/CSHS-CWRA/RavenPy.git>, accessed Jan 2026).

**Table 2.** Description of Raven parameters to emulate HBV and their calibration range.

Raven Parameter	Description	Unit	calibration range
<i>RAINSNOW_TEMP</i>	rain/snow transition temperature	°C	-3 - 3
<i>MELT_FACTOR</i>	maximum snow melt factor	mm d <sup>-1</sup> °C <sup>-1</sup>	2.3 - 10
<i>REFREEZE_FACTOR</i>	maximum refreeze factor	mm d <sup>-1</sup> °C <sup>-1</sup>	0 - 8
<i>SNOW_SWI</i>	water saturation fraction of snow	(-)	0 - 0.2
<i>POROSITY</i>	effective porosity of the soil	(-)	0 - 1
<i>FIELD_CAPACITY</i>	field capacity saturation of the soil	(-)	0.3 - 1
<i>SAT_WILT</i>	minimum saturation	(-)	0 - 0.2
<i>HBV_BETA</i>	HBV infiltration exponent	(-)	0 - 7
<i>MAX_PERC_RATE</i>	percolation rate	mm d <sup>-1</sup>	0.1 - 100
<i>BASEFLOW_COEFF</i>	linear baseflow storage/routing coeff (Fast reservoir)	d <sup>-1</sup>	0.01 - 1
<i>BASEFLOW_COEFF</i>	linear baseflow storage/routing coeff (Slow reservoir)	d <sup>-1</sup>	0.05 - 0.1
<i>BASEFLOW_N</i>	baseflow exponent	(-)	0 - 1
<i>MAX_CAP_RISE_RATE</i>	maximum capillary rise rate	mm d <sup>-1</sup>	0 - 30
<i>TOPSOIL_THICKNESS</i>	soil layer thickness	m	0.01 - 2
<i>TIME_CONC</i>	time of concentration at the unit hydrograph	(-)	0.01 - 6
<i>GLAC_STORAGE_COEFF</i>	maximum linear storage coefficient for glacial melt	(-)	0.05 - 1
<i>PRECIP_CORR</i>	precipitation correction factor	(-)	0.8 - 1.8



### 165 3.3 Coupling approach

Following preprocessing of meteorological forcing and geospatial data for the selected catchment (Figure 2A), GloGEM is calibrated and run by providing a list of RGI v6.0 IDs for glaciers within the catchment boundary. GloGEM provides daily glacier runoff, which includes ice melt, snowmelt, and rainfall from the initially glacierized area based on RGI v6.0 (RGI Consortium, 2017) (Fig. 2B; Huss and Hock, 2018), but does not account for baseflow or runoff–streamflow transformation.

170 For the hydrological model, the catchment is discretized into HRUs based on the DEM, using 100 m elevation bands, landuse class and glacier outlines. It should be noted that HRUs regroup grid cells with similar landuse and elevation, but these grid cells can be spatially disconnected. The number of elevation bands and HRUs for each catchment is provided in the supplementary material (Table S1). Precipitation and temperature inputs for each HRU are derived using spatially weighted averaging of gridded meteorological data from MeteoSwiss products (Fig. 2C). To integrate GloGEM outputs into Raven, we implemented  
175 a one-way coupling in which glacier runoff simulated by GloGEM replaces the precipitation input over glacier-covered areas in Raven.

The Raven model was modified to ensure that glacier runoff is directly added to the runoff-streamflow transfer function, in order to bypass intermediate storage components and preserve the timing and magnitude of glacier contributions. To achieve this, a new land use called *Masked Glacier* is implemented in the model (Fig. 2D). In this model configuration, *Masked Glacier*  
180 land use is defined with zero soil layers to prevent water infiltration into any subsurface storage, and evaporation is set to 0 to avoid any loss to the atmosphere, thereby maintaining the complete glacier runoff signal. Given that ice and snow processes are already accounted for in GloGEM, the air temperature for *Masked Glacier* HRUs is set to 20 °C, thus avoiding any snow accumulation. Lastly, any precipitation corrections are disabled for *Masked Glacier* HRUs. These modifications ensure that glacier contributions are accurately reflected in the simulated streamflow (Fig. 2D).

### 185 3.4 Snow redistribution

We implemented a snow redistribution module in the Raven framework using a simple parameterization similar to SnowSlide (Bernhardt and Schulz, 2010), adapted for semi-distributed models. Snow transport is simulated when a slope threshold and snow-holding depth (depending on slope) are exceeded. The same parametrization as in the FSM2trans snow-hydrological model is used (Quéno et al., 2024), without any additional calibrated parameters. Snow exceeding the holding depth is trans-  
190 ported laterally to neighboring HRUs. In contrast to the original grid-based formulation, where transport weights depend on elevation differences between cells, the semi-distributed approach uses HRU area to weight lateral snow redistribution. To enable this lateral transport, HRU connectivity is derived during catchment preprocessing following the methodology of the HydroBricks modeling framework (Horton and Argentin, 2024). Specifically, surface depressions in the DEM are identified and filled following the method of Wang and Liu (2006). Flow direction and flow accumulation are then computed using the  
195 D8 flow routing algorithm (O’Callaghan and Mark, 1984) as implemented in the Python package pysheds (Bartos, 2020). Flow paths are traced between HRUs, with connection weights based on accumulated upstream area. Disconnected HRUs are linked to the nearest neighbor by centroid distance, ensuring complete catchment connectivity. The resulting connectivity information

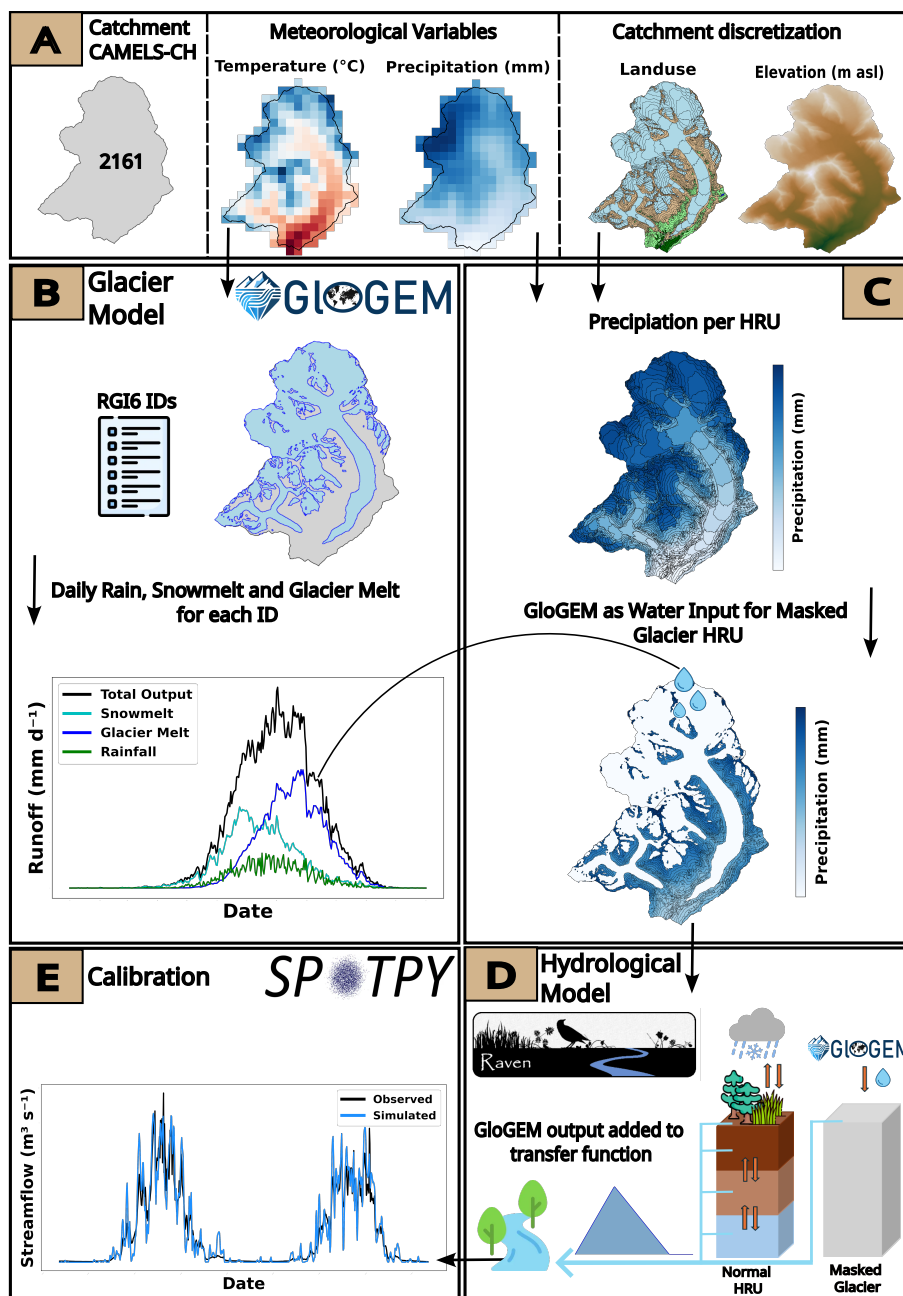


**Figure 2.** Workflow of the coupled GloGEM-Raven configuration. A: Selection of the catchment ID and preprocessing of input data files. B: Calibrating and running the glacier model GloGEM for each glacier in the catchment. C: Calculating precipitation for each HRU and using GloGEM output as water input for glaciated areas. D: Internal mechanism of *Masked Glacier* HRUs adding GloGEM output directly to the triangular transfer function. E: Calibration of the model with Spotpy.



is then provided to Raven as an external input. Depending on the selected configuration, an HRU can be connected either to a single downstream HRU or to multiple HRUs at lower elevations.

### 200 3.5 Calibration

GloGEM is calibrated to match simulated glacier-specific mass balance with observed geodetic mass balance from Hugonnet et al. (2021), aiming to reproduce the long-term trend of glacier evolution for each individual glacier over the period 2000–2019 (Zekollari et al., 2024). Throughout calibration, the glacier area is kept constant. Three parameters are optimized sequentially:  $f_{c,prec}$ , a multiplicative precipitation correction factor;  $f_{dd,snow}$ , the degree-day factor for snow (with  $f_{dd,ice} = 2f_{dd,snow}$ ), which  
 205 links air temperature to melt rates; and  $f_{t,offset}$ , a local temperature correction term. Initial estimates are  $f_{c,prec} = 0.8$  (range: 0.8–5.0),  $f_{dd,snow} = 3 \text{ mm d}^{-1} \text{ } ^\circ\text{C}^{-1}$  (range: 1.75–4.5), and  $f_{t,offset} = 0 \text{ } ^\circ\text{C}$  (Hock, 2003). The calibration is carried out in three sequential phases: first,  $f_{c,prec}$  is adjusted to account for precipitation uncertainty and local orographic effects; if the target tolerance is not achieved,  $f_{dd,snow}$  is optimized while keeping  $f_{c,prec}$  constant; finally, if necessary,  $f_{t,offset}$  is adjusted to correct systematic temperature biases. Convergence is considered achieved when the difference between simulated and observed mass  
 210 balance falls within a predefined tolerance, set arbitrarily between 0.01 and 0.05 m w.e.  $\text{a}^{-1}$  (Zekollari et al., 2024).

The Raven calibration routine is established using the Python Spotpy package (Houska et al., 2015) (Fig. 2E). The Shuffled Complex Evolution (SCE-UA) algorithm is used for the calibration process (Duan et al., 1993). The number of iterations to achieve convergence is set to 10000 and the number of complexes is 15. In this study, all selected catchments are calibrated for the period 1 January 2000 to 31 December 2009 and evaluated from 1 January 2010 to 31 December 2020. The objec-  
 215 tive function used is the Kling-Gupta Efficiency (KGE; Gupta et al., 2009), which contains correlation, bias, and variability components.

**Table 3.** Model configurations and number of calibrated parameters used in this study.

Model configuration	GloGEM	Snow Redistribution (SR)	Precipitation Correction Factor (PCF)	# parameters
HBV	×	×	×	15
HBV-SR	×	✓	×	15
HBV-PCF	×	✓	✓	16
HBV-GloGEM	✓	×	×	14
HBV-GloGEM-SR	✓	✓	×	14
HBV-GloGEM-PCF	✓	✓	✓	15

Six model configurations are calibrated for each catchment (Table 3). The first three configurations use the native HBV glacier module: (1) baseline HBV with 15 calibrated parameters, (2) HBV with snow redistribution (HBV-SR, 15 parameters), and (3) HBV with snow redistribution and a calibrated precipitation correction factor (HBV-PCF, 16 parameters). The  
 220 remaining three configurations employ the coupled models: (4) HBV-GloGEM, (5) HBV-GloGEM-SR with snow redistribu-



tion, and (6) HBV-GloGEM-PCF with snow redistribution and precipitation correction. The coupled configurations require one parameter less since the linear glacier outflow parameter of HBV's glacier model is not used.

## 4 Results

### 4.1 Streamflow performance

225 Model performance is evaluated using KGE (Gupta et al., 2009), which also serves as the calibration objective function, and the Nash-Sutcliffe Efficiency (NSE; Nash and Sutcliffe, 1970). KGE and NSE are computed based on daily simulated and observed streamflow. Figure 3a presents KGE and NSE values for all catchments over the validation period. The KGE results indicate that uncoupled HBV configurations slightly outperform coupled configurations, with median KGE values for HBV configurations ranging between 0.83 and 0.86 compared to median KGE values ranging from 0.81 to 0.84 for HBV-GloGEM configurations. In terms of NSE, the two configurations show relatively similar performance, with median values of 0.78–0.79 for HBV and 0.77–0.78 for HBV-GloGEM. Model performance is generally similar with the addition of snow redistribution. The application of a precipitation correction factor improves KGE and NSE for most catchments. A table with all KGE and NSE values is provided in the supplementary material (Table S2 and Table S3).

235 Figure 3b illustrates streamflow regimes, glacier melt, and snowmelt for the validation period in two representative catchments. The left column shows simulations compared to observed streamflow for the Rhone catchment, which has a glacierized area of 44.1 % in the year 2000. The standard HBV configuration overestimates late-season streamflow and underestimates early melt season discharge, which was found across many study catchments. Snow redistribution partially addresses this issue. The coupled HBV-GloGEM model better captures late-summer streamflow, but fails to reproduce peak summer discharge without precipitation correction. The Alpbach catchment (right column), which has a glacierized area of 22.1 % in the year 2000, exhibits similar temporal biases, with underestimated early-season and overestimated late-season streamflow. The HBV-GloGEM and HBV-GloGEM-SR configurations struggle to reproduce observed streamflow due to insufficient water availability. However, incorporating a precipitation correction factor substantially improves model performance. The different model configurations produce substantially different glacier melt and snowmelt dynamics, both in magnitude and seasonal timing, with the strongest contrasts observed in the less glacierized Alpbach catchment.

### 245 4.2 Glacier melt

To evaluate the simulated glacier melt, we use the glacier melt dataset for Switzerland described in van Tiel et al. (2025), hereafter referred to as the reference melt. The results show that GloGEM reproduces the reference melt more accurately than the hydrological model (Figure 4). The HBV glacier module consistently overestimates melt, except in catchments with very low glacier cover such as the Goneri and Reuss. Incorporating snow redistribution in the model often reduces simulated HBV melt, bringing results closer to the reference melt in catchments where overestimation occurs. This effect is particularly noticeable in the highly glaciated Massa catchment, where the HBV-SR configuration agrees well with the reference melt.

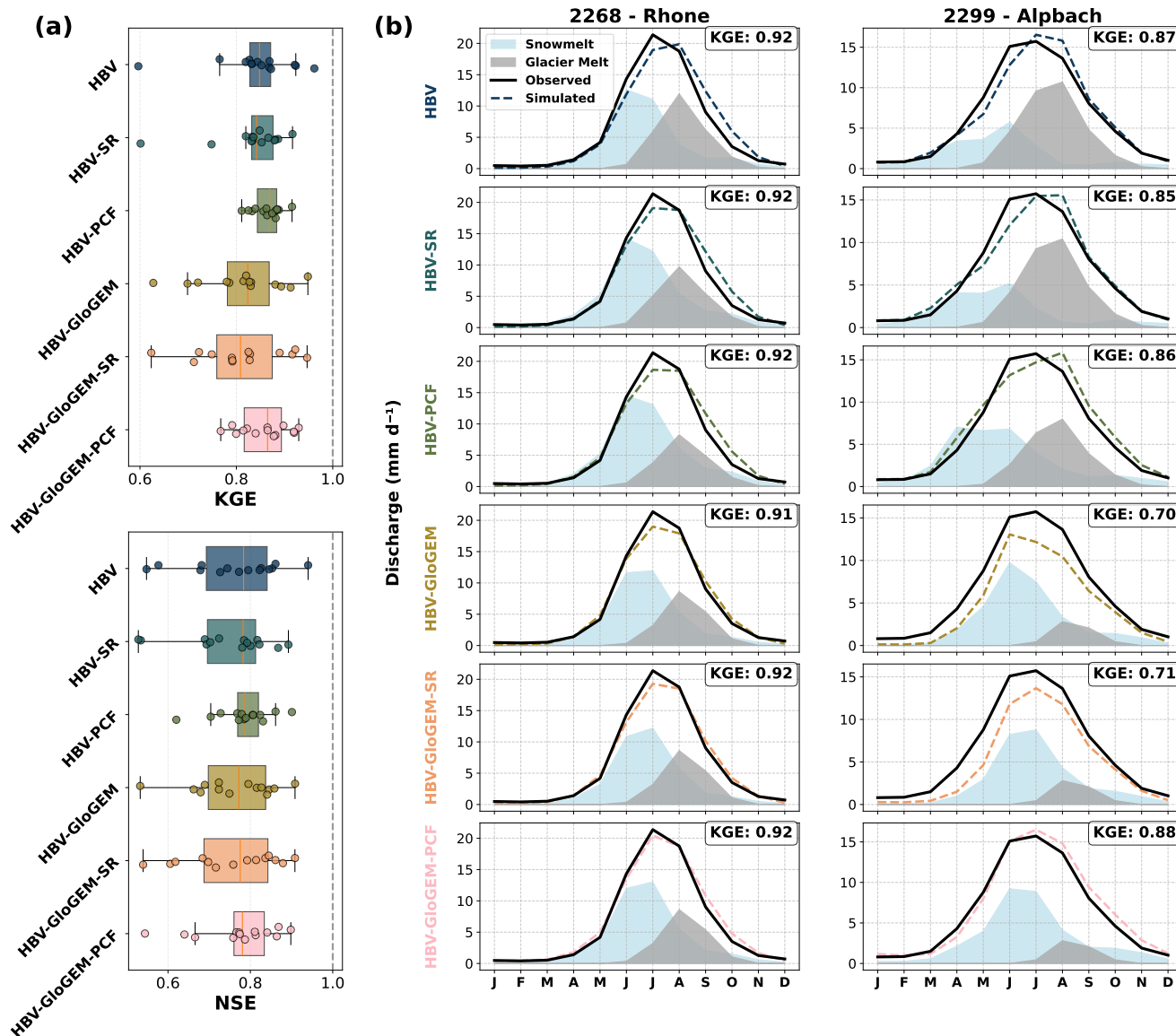


**Figure 3.** (a) KGE and NSE values for the validation period for all configurations and all catchments are shown in a boxplot. (b) Streamflow regime (monthly averaged values), glacier melt regime and snowmelt regime during the entire validation period for all configurations and two representative catchments, Rhone (ID 2268) and Alpbach (ID 2299).

Introducing a precipitation correction factor further reduces simulated melt in most catchments; for example, in the Simme catchment, the HBV glacier module reproduces the reference melt well when the correction factor is applied (HBV-PCF). However, overestimation remains in most catchments. As GloGEM uses geodetic mass balance for calibration, it is expected to better reproduce the glacier mass balance across Switzerland.

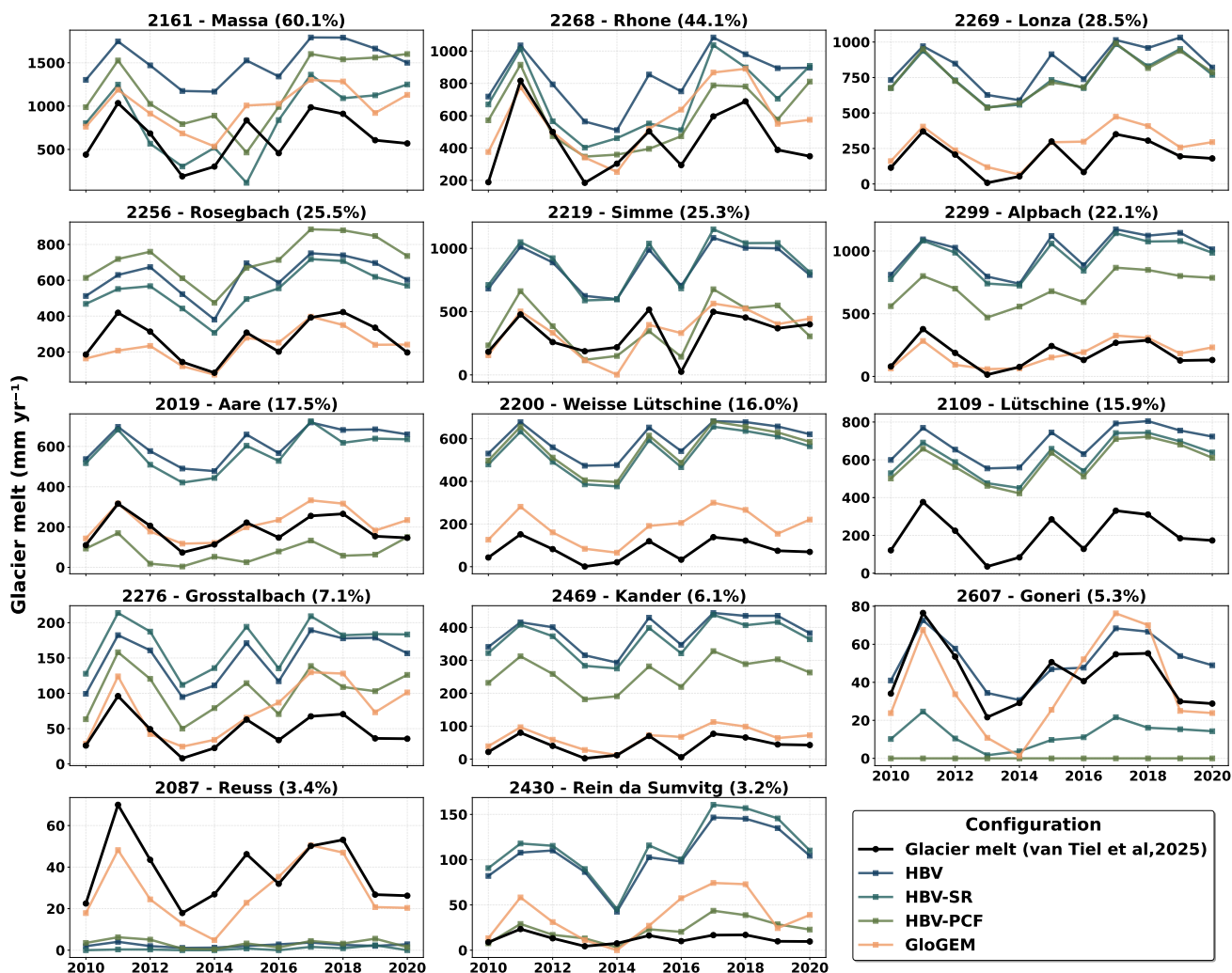


**Figure 4.** Glacier melt (van Tiel et al., 2025) and simulated glacier melt for 14 Swiss catchments, the different HBV configurations, and GloGEM.

### 4.3 SWE performance

Simulated catchment-average snow water equivalent (SWE) was validated against the 1 km gridded SPASS dataset (Marty et al., 2025) (Figure 5). The root mean square error (RMSE) is computed based on the daily catchment average SWE (only non-glacier area) of the SPASS dataset and simulated SWE. In the HBV and HBV-GloGEM configurations, the simulations show a continuous increase in catchment-average SWE, indicating unrealistic snow accumulation in higher-elevation HRUs (Freudiger et al., 2017). The median RMSE is 243 mm and 184 mm, respectively, suggesting that catchment-average SWE is poorly represented when snow redistribution is not included in the model. Incorporating snow redistribution substantially



improves the representation of catchment-average SWE, as seen for HBV-SR with an average RMSE of 142 mm and for HBV-GloGEM-SR with an average RMSE of 134 mm, showing strong agreement with the SPASS dataset. When applying a precipitation correction factor, SWE remains well represented for the HBV-PCF configuration (145 mm) but deteriorates for the HBV-GloGEM-PCF configuration (166 mm). The latter generally requires a higher precipitation correction factor (Figure S22), which can result in excessive snow input and consequently reduces model performance for SWE.

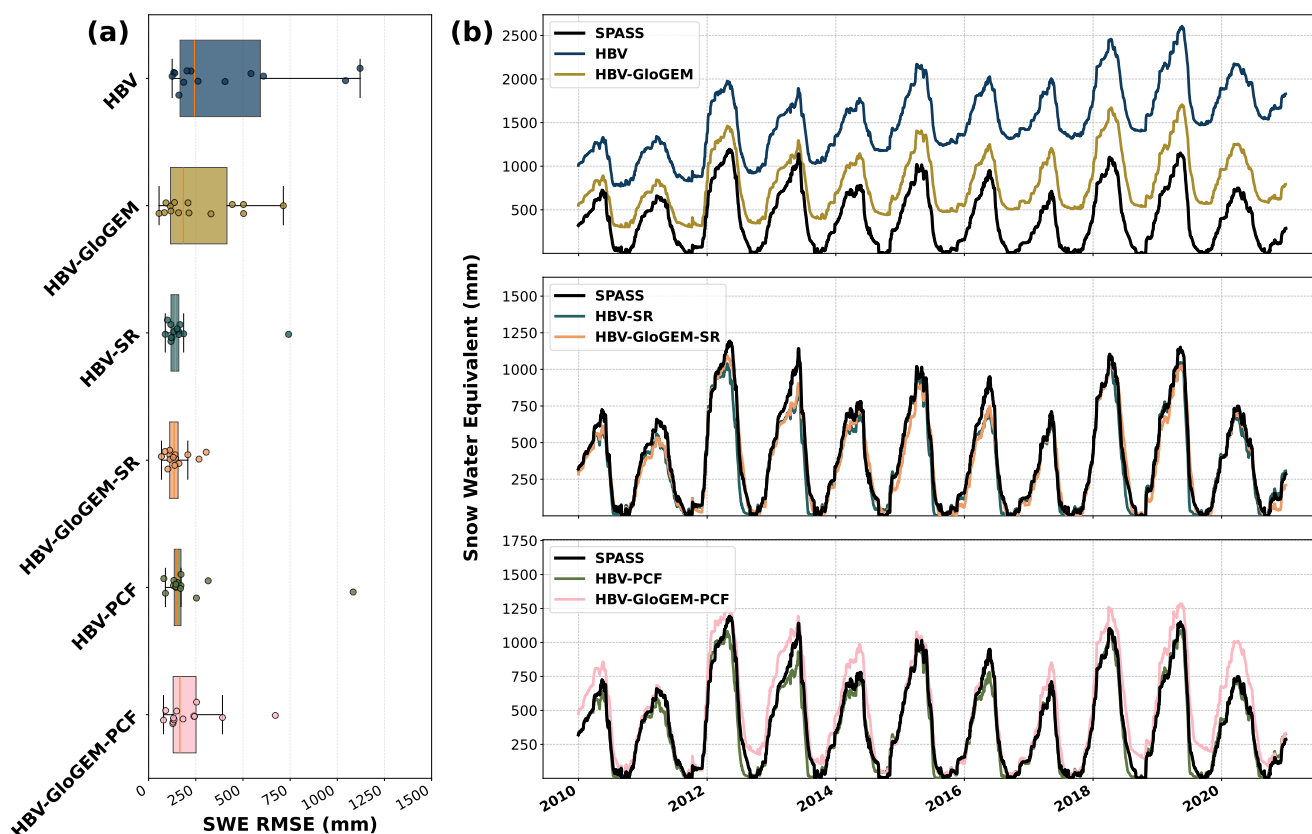


**Figure 5.** (a) Catchment average (non-glacier area) SWE performance calculated with RMSE for all catchments and configurations. (b) Time series of catchment average (non-glacier area) SWE in the validation period for the Rhone catchment (ID 2268) and all six model configurations.

#### 4.4 Model parameters

Calibrating the model under different configurations leads to shifts in parameter distributions, particularly for snow and melt parameters. Figure 6 presents the melt factor in  $\text{mm } ^\circ\text{C}^{-1} \text{ d}^{-1}$  for the 100 best parameter sets across the eight most glaciated catchments, for which the model coupling has the strongest influence on parameter behavior. Coupling HBV with GloGEM produces the largest shifts in melt factor values compared to the original HBV configurations, consistently resulting in lower



calibrated melt factors. Including snow redistribution has little influence on the melt factor, while the precipitation correction factor affects melt parameters only in a small number of catchments. Parameter distribution plots for all snow-related parameters are provided in the Supplementary Material (Figures S19–S22).

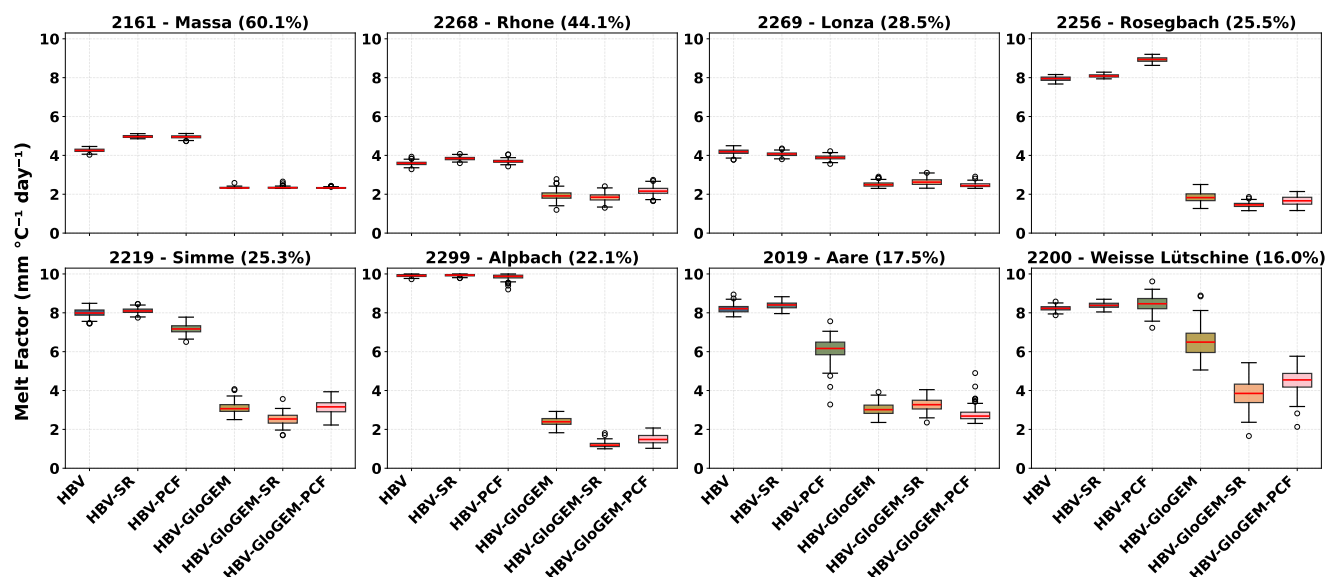


**Figure 6.**  $f_{\text{MELT\_FACTOR}}$  parameter distribution for the 8 most glaciated catchments and all model configurations.

## 4.5 Uncertainty

Applying a precipitation correction factor improves streamflow performance but also increases the uncertainty in estimating glacier and snowmelt contributions. Figure 7a illustrates the streamflow, glacier melt, and snowmelt regimes for the 20 best parameter sets for the Rhone catchment. The Rhone catchment exemplifies equifinality, where multiple parameter sets yield similarly good streamflow performance but substantially different melt dynamics. For the HBV-PCF configuration, simulated annual glacier melt contributions range from 11 % to 38 %, while snowmelt contributions vary between 51 % and 73 %.

Figure 7b shows the coefficient of variation (CV) in melt estimates for the eight catchments with the highest glacier coverage. Catchments with very little glacier melt are not shown, as CV values in those catchments become extremely high and do not reflect meaningful variability. The CV of glacier melt is markedly higher for the HBV-PCF configuration than for the other HBV setups, reflecting increased sensitivity when a precipitation correction factor is applied. As expected, GloGEM configurations show no variation in glacier melt because it is provided as a fixed input. Snowmelt uncertainty also rises under the HBV-PCF configuration, reaching its highest values in the most glaciated catchments.

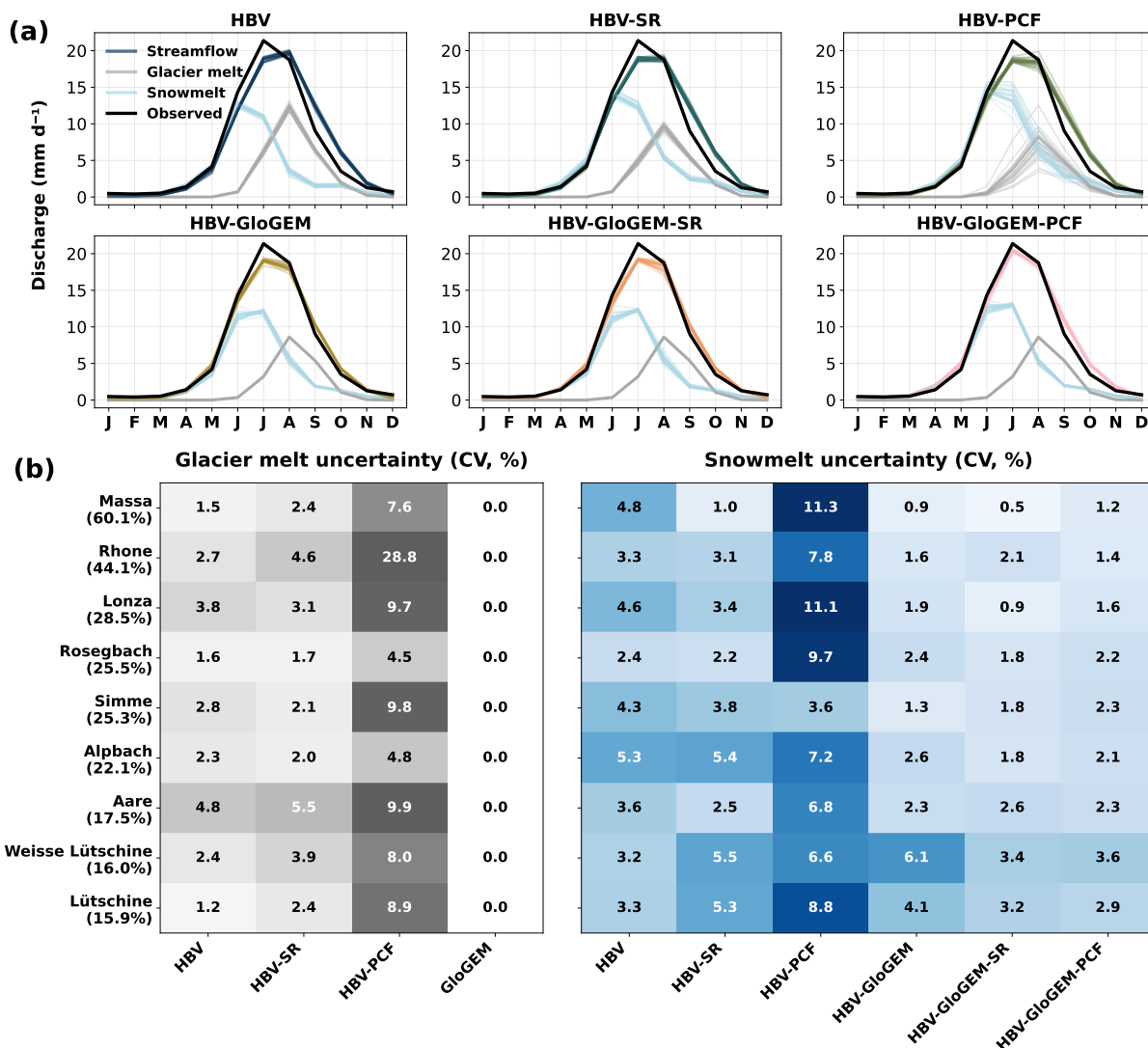


**Figure 7.** (a) Streamflow regimes, glacier melt regimes and snowmelt regimes for the validation period for all configurations for the 20 best parameter sets in the Rhone (ID 2268) catchment. (b) The coefficient of variation (CV) calculated for most glaciated catchments and all configurations for annual snowmelt and glacier melt.

#### 4.6 Annual contributions

Annual melt contributions vary substantially across model configurations within each catchment (Figure 8). For HBV configurations, snow redistribution has a pronounced effect: snowmelt contributions increase and glacier melt decreases in most catchments, while total melt remains relatively constant. This is expected, as snow redistribution allows snow that was previously inaccessible in 'snow towers', to become available for melt. The impact of precipitation correction on annual melt



partitioning is configuration-dependent and lacks a consistent directional pattern. For instance, in the Massa catchment, precipitation correction increases glacier melt contributions, whereas in the Simme catchment it substantially reduces glacier melt, bringing simulations into close agreement with the reference melt contributions (van Tiel et al., 2025). In contrast, snow redistribution has minimal impact on melt partitioning in HBV-GloGEM configurations. However, precipitation correction consistently increases snowmelt contributions across most catchments in the coupled model. Comparing glacier representations, HBV-GloGEM configurations generally reproduce the reference glacier melt contributions well, whereas HBV configurations systematically overestimate glacier melt across catchments.

## 300 5 Discussion

In this study, we coupled the hydrological modeling framework Raven (Craig et al., 2020), emulating HBV, with the Global Glacier Evolution Model GloGEM (Huss and Hock, 2015) and implemented a snow redistribution scheme to improve process representation in 14 glaciated catchments across the Swiss Alps. We investigated whether introducing additional constraints through glacier model coupling and improved snow distribution could reduce parameter equifinality and improve the quantification of seasonal snow and glacier melt contributions.

The uncoupled HBV configurations consistently outperformed the coupled HBV-GloGEM setups according to calculated streamflow metrics (KGE and NSE). This contrasts with findings from recent coupling studies that reported improved streamflow simulations when integrating global glacier models (Wiersma et al., 2022; Hanus et al., 2024). However, these studies coupled global glacier models with global hydrological models that previously lacked any glacier representation. Only Pesci et al. (2023) compared a coupled model against a traditional volume-area scaling approach, finding similar streamflow performance in a single Austrian catchment. Our results across 14 Swiss catchments reveal more complex patterns, with some catchments showing comparable performance between configurations while others exhibiting substantial discrepancies.

While original HBV configurations achieve better streamflow metrics, they do so by simulating glacier melt rates that exceed both GloGEM estimates and the reference glacier mass loss (van Tiel et al., 2025) by factors of two to three in some catchments. The HBV glacier module provides additional degrees of freedom during calibration, allowing the glacier component to compensate for various model deficiencies, including process representation limitations and input data biases (Duethmann et al., 2015; He et al., 2015). This compensation primarily results from precipitation underestimation in the forcing data, a challenge in complex mountain terrain where spatial interpolation errors can be substantial (Immerzeel et al., 2014; Henn et al., 2018). To a lesser extent, uncertainties in solid-liquid precipitation partitioning may also influence model behavior (Magnusson et al., 2011). The HBV glacier model responds to these deficiencies by amplifying melt rates during calibration, effectively using glacier ice as an adjustment variable to close the water balance.

This compensation mechanism is particularly problematic when attempting to quantify individual melt contributions. A key challenge is parameter equifinality (Beven, 2006), where multiple parameter combinations can produce equally good streamflow simulations while implying vastly different snow and glacier melt estimates. Without precipitation correction, HBV systematically overestimates glacier melt. With precipitation correction included, the model gains an additional degree of

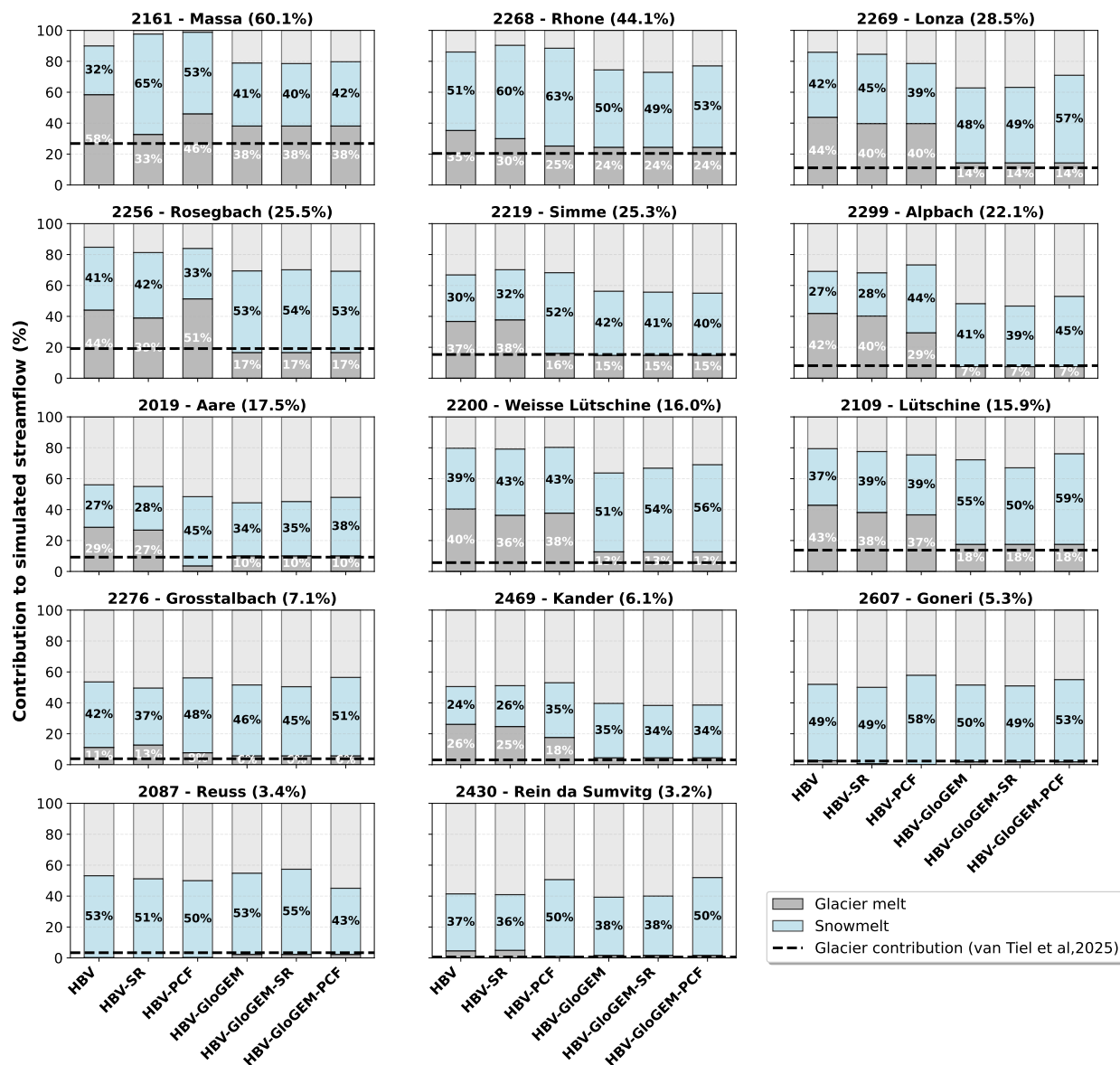


**Figure 8.** Annual contributions from glacier and snowmelt in % to the annual streamflow for all catchments and each configuration.

freedom, creating trade-offs between the precipitation correction factor and glacier melt parameters. Stahl et al. (2008) showed that equivalent streamflow simulations can correspond to widely varying glacier mass balance estimates. Our uncertainty analysis confirms this pattern, where among the 20 best-performing parameter sets, simulated glacier melt contributions vary substantially. This has important implications for climate impact studies. Models that perform well due to compensating errors



330 may misrepresent key components of the present-day water balance. As a result, they are unlikely to provide reliable projections under future conditions as melt contributions to streamflow shift under a changing climate.

Coupling with GloGEM provides glacier evolution calibrated to observed geodetic mass balance (Hugonnet et al., 2021), resulting in glacier melt estimates that align with the reference glacier mass loss across Switzerland. However, glacier model calibration itself is subject to equifinality, as multiple parameter combinations can reproduce the observed geodetic mass  
335 balance (Gabbi et al., 2014; Von Der Esch et al., 2025). Calibration to geodetic mass balance remains the most widely applied method for global glacier models (Rounce et al., 2023; Zekollari et al., 2024), as this data is consistently available for glaciers worldwide. Despite inherent uncertainties in glacier model parameters, the simulated glacier melt corresponds closer to the reference glacier melt than the HBV glacier melt.

Beyond constraining glacier evolution, accurately representing snowmelt contributions requires realistic simulation of snow  
340 accumulation patterns in complex mountain terrain. Snow redistribution processes remain poorly represented in glacio-hydrological modeling, with van Tiel et al. (2020) finding that only 20% of published studies explicitly account for these processes. Neglecting snow redistribution results in unrealistic snow accumulation at high elevations, as observed in most catchments in this study. Our implementation uses a simplified gravitational redistribution scheme (Freudiger et al., 2017), a common approach in hydrological modeling that does not simulate the actual physical processes of wind drift and avalanches. Despite this sim-  
345 plification, the snow redistribution scheme successfully prevents unrealistic snow tower formation (Frey and Holzmann, 2015) and improves melt partitioning. Redistributing snow to lower, warmer elevations increases the proportion of melt originating from snow rather than glacier ice, producing more physically consistent melt contributions that align better with observations.

Future work could further reduce parameter equifinality by incorporating additional observational constraints beyond geode-  
350 tic mass balance and streamflow. Glacier model calibration could be refined using seasonal snowline observations, which provide stronger constraints on glacier ablation patterns than annual mass balance alone (Barandun et al., 2018; Cremona et al., 2025). Similarly, remote sensing snow cover products offer potential for constraining the hydrological model's snow accumulation and melt processes (Parajka and Blöschl, 2008; Di Marco et al., 2021). However, given that constraining glacier evolution already substantially improves snowmelt identifiability through reduced compensatory adjustments, the marginal benefit of additional snow cover constraints requires further investigation.

## 355 6 Conclusions

Mountain regions face substantial hydrological changes as climate warming alters snow and glacier melt dynamics. Accurately projecting these changes requires hydrological models that correctly partition melt contributions between snow and glacier sources. This study investigated whether coupling the hydrological model Raven with the Global Glacier Evolution Model GloGEM and implementing snow redistribution could reduce parameter equifinality and improve melt contribution estimates.  
360 We applied this framework to 14 headwater catchments in Switzerland, comparing six model configurations that varied in glacier representation, snow redistribution, and precipitation correction. Our analysis reveals a fundamental challenge: models achieving superior calibration performance do not necessarily provide accurate process representation. While uncoupled



HBV configurations outperformed coupled HBV-GloGEM setups by streamflow metrics, they did so by simulating glacier melt 2-3 times higher than reference datasets to compensate for precipitation biases in the forcing data. Applying a precipitation correction factor produced severe parameter equifinality, with glacier melt varying substantially between equally well performing parameter sets. Coupling with GloGEM, constrained by geodetic mass balance, improved the identifiability of both melt components while simulating glacier melt consistent with the reference dataset. Snow redistribution further enhances model reliability by addressing unrealistic accumulation patterns. For mountain hydrology under climate change, these results carry important implications. Models calibrated solely on streamflow can achieve good historical performance while misrepresenting the processes that determine future behavior. This is a critical limitation as warming alters melt dynamics. Our work demonstrates that coupling a hydrological model with a global glacier model provides a more reliable framework for climate impact assessments, even though this results in a minor reduction in historical performance metrics. Future advances could integrate additional constraints, such as seasonal snowline observations or snow cover products, to further increase the identifiability of melt contributions.

*Code and data availability.* Meteorological data are available through MeteoSwiss (<https://opendatadocs.meteoswiss.ch/c-climate-data/c7-spatial-climate-normals>). The streamflow data is available through CAMELS-CH (<https://doi.org/10.5281/zenodo.7784632>, Höge et al. (2023)). SPASS dataset for daily gridded SWE is available through <https://envidat.ch> (<https://doi.org/10.16904/envidat.580>, Marty et al. (2025)). The glacier storage data for all glaciers in Switzerland is available at <https://doi.org/10.3929/ethz-c-000786939> (Van Tiel and Huss, 2025). The modified Raven model is available at (<https://github.com/bergjus94/RavenHydro.git>). The GitHub repository for the coupling workflow will be made available upon publication. This will also contain the full simulation results.

*Author contributions.* J.B. designed the study, implemented the model developments, performed the simulations and analyses, and wrote the original manuscript. P.H. provided guidance on model development. P.H. and M.K. co-designed the study and supervised the work. P.H., M.K. and B.S. . P.H. and M.K. acquired the project funds. A.E. provided the glacier model output and advice on its further use for hydrological modeling. B.S provided critical input on the study design, results analysis, and interpretation. All authors contributed to manuscript revision and approved the final version.

*Competing interests.* The authors declare that they have no conflict of interest.

*Acknowledgements.* The work of J.B. was funded through the Swiss National Science Foundation project IZINZ2\_209531 entitled "21st cEnTury Evolution of small glacieRs and their impact on regioNAL hydrology in the HIMAlayas (ETERNALHIMA)".



## References

- 390 Arnoux, M., Brunner, P., Schaefli, B., Mott, R., Cochand, F., and Hunkeler, D.: Low-flow behavior of alpine catchments with varying quaternary cover under current and future climatic conditions, *Journal of Hydrology*, 592, 125 591, <https://doi.org/10.1016/j.jhydrol.2020.125591>, 2021.
- Bahr, D. B., Meier, M. F., and Peckham, S. D.: The physical basis of glacier volume-area scaling, *Journal of Geophysical Research: Solid Earth*, 102, 20 355–20 362, <https://doi.org/10.1029/97JB01696>, 1997.
- 395 Barandun, M., Huss, M., Usabaliyev, R., Azisov, E., Berthier, E., Käab, A., Bolch, T., and Hoelzle, M.: Multi-decadal mass balance series of three Kyrgyz glaciers inferred from modelling constrained with repeated snow line observations, *The Cryosphere*, 12, 1899–1919, <https://doi.org/10.5194/tc-12-1899-2018>, 2018.
- Bartos, M.: pysheds: Simple and Fast Watershed Delineation in Python, <https://github.com/mdbartos/pysheds>, 2020.
- Bergström, S.: The HBV Model, no. 4 in SMHI Reports Hydrology, Swedish Meteorological and Hydrological Institute, Norrköping, Sweden, 43 pages, 1995.
- 400 Bernhardt, M. and Schulz, K.: SnowSlide: A simple routine for calculating gravitational snow transport, *Geophysical Research Letters*, 37, 2010GL043 086, <https://doi.org/10.1029/2010GL043086>, 2010.
- Beven, K.: A manifesto for the equifinality thesis, 320, 18–36, <https://doi.org/10.1016/j.jhydrol.2005.07.007>, 2006.
- Biemans, H., Siderius, C., Lutz, A. F., Nepal, S., Ahmad, B., Hassan, T., Von Bloh, W., Wijngaard, R. R., Wester, P., Shrestha, A. B., and Immerzeel, W. W.: Importance of snow and glacier meltwater for agriculture on the Indo-Gangetic Plain, *Nature Sustainability*, 2, 594–601, <https://doi.org/10.1038/s41893-019-0305-3>, 2019.
- 405 Craig, J. R.: Raven: User’s and Developer’s Manual v4.0, <http://raven.uwaterloo.ca/>, raven Development Team. Accessed December 2025, 2025.
- Craig, J. R., Brown, G., Chlumsky, R., Jenkinson, R. W., Jost, G., Lee, K., Mai, J., Serrer, M., Sgro, N., Shafii, M., Snowdon, A. P., and Tolson, B. A.: Flexible watershed simulation with the Raven hydrological modelling framework, *Environmental Modelling & Software*, 129, <https://doi.org/10.1016/j.envsoft.2020.104728>, 2020.
- 410 Cremona, A., Huss, M., Landmann, J. M., Schwaizer, G., Paul, F., and Farinotti, D.: Constraining sub-seasonal glacier mass balance in the Swiss Alps using Sentinel-2-derived snow-cover observations, *Journal of Glaciology*, 71, e25, <https://doi.org/10.1017/jog.2025.1>, 2025.
- Di Marco, N., Avesani, D., Righetti, M., Zaramella, M., Majone, B., and Borga, M.: Reducing hydrological modelling uncertainty by using MODIS snow cover data and a topography-based distribution function snowmelt model, *Journal of Hydrology*, 599, 126 020, <https://doi.org/10.1016/j.jhydrol.2021.126020>, 2021.
- 415 Duan, Q. Y., Gupta, V. K., and Sorooshian, S.: Shuffled complex evolution approach for effective and efficient global minimization, *Journal of Optimization Theory and Applications*, 76, 501–521, <https://doi.org/10.1007/BF00939380>, 1993.
- Duethmann, D., Bolch, T., Farinotti, D., Kriegel, D., Vorogushyn, S., Merz, B., Pieczonka, T., Jiang, T., Su, B., and Güntner, A.: Attribution of streamflow trends in snow and glacier melt-dominated catchments of the *T* arim *R* iver, *Central Asia*, 51, 4727–4750, <https://doi.org/10.1002/2014WR016716>, 2015.
- 420 ESA WorldCover: ESA WorldCover 10m 2021, Version 2.0, <https://worldcover2020.esa.int/>, accessed: 2024-06-21, 2021.
- Farinotti, D., Usselman, S., Huss, M., Bauder, A., and Funk, M.: Runoff evolution in the Swiss Alps: projections for selected high-alpine catchments based on *ENSEMBLES* scenarios, *Hydrological Processes*, 26, 1909–1924, <https://doi.org/10.1002/hyp.8276>, 2012.
- 425



- Frei, P., Kotlarski, S., Liniger, M. A., and Schär, C.: Future snowfall in the Alps: projections based on the EURO-CORDEX regional climate models, *The Cryosphere*, 12, 1–24, <https://doi.org/10.5194/tc-12-1-2018>, 2018.
- Freudiger, D., Kohn, I., Seibert, J., Stahl, K., and Weiler, M.: Snow redistribution for the hydrological modeling of alpine catchments, *WIREs Water*, 4, e1232, <https://doi.org/10.1002/wat2.1232>, 2017.
- 430 Frey, S. and Holzmann, H.: A conceptual, distributed snow redistribution model, *Hydrology and Earth System Sciences*, 19, 4517–4530, <https://doi.org/10.5194/hess-19-4517-2015>, 2015.
- Gabbi, J., Carenzo, M., Pellicciotti, F., Bauder, A., and Funk, M.: A comparison of empirical and physically based glacier surface melt models for long-term simulations of glacier response, *Journal of Glaciology*, 60, 1140–1154, <https://doi.org/10.3189/2014JoG14J011>, 2014.
- Gupta, H. V., Kling, H., Yilmaz, K. K., and Martinez, G. F.: Decomposition of the mean squared error and NSE performance criteria: Implications for improving hydrological modelling, *Journal of Hydrology*, 377, 80–91, <https://doi.org/10.1016/j.jhydrol.2009.08.003>, 2009.
- 435 HADES: Hydrological Atlas of Switzerland, Data and Analysis Platform, [https://hydromaps.ch/#de/8/46.830/8.193/bl\\_hds](https://hydromaps.ch/#de/8/46.830/8.193/bl_hds), accessed: Nov. 12, 2025, 2025.
- Han, J., Liu, Z., Woods, R., McVicar, T. R., Yang, D., Wang, T., Hou, Y., Guo, Y., Li, C., and Yang, Y.: Streamflow seasonality in a snow-dwindling world, *Nature*, 629, 1075–1081, <https://doi.org/10.1038/s41586-024-07299-y>, 2024.
- 440 Hanus, S., Schuster, L., Burek, P., Maussion, F., Wada, Y., and Viviroli, D.: Coupling a large-scale glacier and hydrological model (OGGM v1.5.3 and CWatM V1.08) – Towards an improved representation of mountain water resources in global assessments, <https://doi.org/10.5194/egusphere-2023-2562>, 2024.
- Hanzer, F., Förster, K., Nemeč, J., and Strasser, U.: Projected cryospheric and hydrological impacts of 21st century climate change in the Ötztal Alps (Austria) simulated using a physically based approach, *Hydrology and Earth System Sciences*, 22, 1593–1614, <https://doi.org/10.5194/hess-22-1593-2018>, 2018.
- 445 He, Z. H., Tian, F. Q., Gupta, H. V., Hu, H. C., and Hu, H. P.: Diagnostic calibration of a hydrological model in a mountain area by hydrograph partitioning, *Hydrology and Earth System Sciences*, 19, 1807–1826, <https://doi.org/10.5194/hess-19-1807-2015>, 2015.
- Henn, B., Newman, A. J., Livneh, B., Daly, C., and Lundquist, J. D.: An assessment of differences in gridded precipitation datasets in complex terrain, *Journal of Hydrology*, 556, 1205–1219, <https://doi.org/10.1016/j.jhydrol.2017.03.008>, 2018.
- 450 Hock, R.: Temperature index melt modelling in mountain areas, *Journal of Hydrology*, 282, 104–115, [https://doi.org/10.1016/S0022-1694\(03\)00257-9](https://doi.org/10.1016/S0022-1694(03)00257-9), 2003.
- Horton, P. and Argentin, A.-L.: Hydrobricks, <https://doi.org/10.5281/zenodo.11082505>, 2024.
- Horton, P., Schaeffli, B., Mezghani, A., Hingray, B., and Musy, A.: Assessment of climate-change impacts on alpine discharge regimes with climate model uncertainty, *Hydrological Processes*, 20, 2091–2109, <https://doi.org/10.1002/hyp.6197>, 2006.
- 455 Houska, T., Kraft, P., Chamorro-Chavez, A., and Breuer, L.: SPOTting Model Parameters Using a Ready-Made Python Package, *PLOS ONE*, 10, e0145180, <https://doi.org/10.1371/journal.pone.0145180>, 2015.
- Hugonnet, R., McNabb, R., Berthier, E., Menounos, B., Nuth, C., Girod, L., Farinotti, D., Huss, M., Dussailant, I., Brun, F., and Käab, A.: Accelerated global glacier mass loss in the early twenty-first century, *Nature*, 592, 726–731, <https://doi.org/10.1038/s41586-021-03436-z>, 2021.
- 460 Huss, M. and Hock, R.: A new model for global glacier change and sea-level rise, *Front. Earth Sci.*, 3, <https://doi.org/10.3389/feart.2015.00054>, 2015.
- Huss, M. and Hock, R.: Global-scale hydrological response to future glacier mass loss, 8, 135–140, <https://doi.org/10.1038/s41558-017-0049-x>, 2018.



- Huss, M., Juvet, G., Farinotti, D., and Bauder, A.: Future high-mountain hydrology: a new parameterization of glacier retreat, *465* <https://doi.org/10.5194/hessd-7-345-2010>, 2010.
- Höge, M., Kauzlaric, M., Siber, R., Schönenberger, U., Horton, P., Schwanbeck, J., Floriancic, M. G., Viviroli, D., Wilhelm, S., Sikorska-Senoner, A. E., Addor, N., Brunner, M., Pool, S., Zappa, M., and Fenicia, F.: CAMELS-CH: hydro-meteorological time series and landscape attributes for 331 catchments in hydrologic Switzerland, *Earth System Science Data*, 15, 5755–5784, <https://doi.org/10.5194/essd-15-5755-2023>, 2023.
- 470 Immerzeel, W. W., Petersen, L., Ragetti, S., and Pellicciotti, F.: The importance of observed gradients of air temperature and precipitation for modeling runoff from a glacierized watershed in the Nepalese Himalayas, *Water Resources Research*, 50, 2212–2226, <https://doi.org/10.1002/2013WR014506>, 2014.
- Immerzeel, W. W., Lutz, A. F., Andrade, M., Bahl, A., Biemans, H., Bolch, T., Hyde, S., Brumby, S., Davies, B. J., Elmore, A. C., Emmer, A., Feng, M., Fernández, A., Haritashya, U., Kargel, J. S., Koppes, M., Kraaijenbrink, P. D. A., Kulkarni, A. V., Mayewski, P. A., Nepal, 475 S., Pacheco, P., Painter, T. H., Pellicciotti, F., Rajaram, H., Rupper, S., Sinisalo, A., Shrestha, A. B., Viviroli, D., Wada, Y., Xiao, C., Yao, T., and Baillie, J. E. M.: Importance and vulnerability of the world’s water towers, *Nature*, 577, 364–369, <https://doi.org/10.1038/s41586-019-1822-y>, 2020.
- Jansson, P., Hock, R., and Schneider, T.: The concept of glacier storage: a review, *Journal of Hydrology*, 282, 116–129, [https://doi.org/10.1016/S0022-1694\(03\)00258-0](https://doi.org/10.1016/S0022-1694(03)00258-0), 2003.
- 480 Kaser, G., Großhauser, M., and Marzeion, B.: Contribution potential of glaciers to water availability in different climate regimes, *Proceedings of the National Academy of Sciences*, 107, 20 223–20 227, <https://doi.org/10.1073/pnas.1008162107>, 2010.
- Magnusson, J., Farinotti, D., Jonas, T., and Bavay, M.: Quantitative evaluation of different hydrological modelling approaches in a partly glacierized Swiss watershed, *Hydrological Processes*, 25, 2071–2084, <https://doi.org/10.1002/hyp.7958>, 2011.
- Magnusson, J., Gustafsson, D., Hüsler, F., and Jonas, T.: Assimilation of point SWE data into a distributed snow cover model comparing two 485 contrasting methods, *Water Resources Research*, 50, 7816–7835, <https://doi.org/10.1002/2014WR015302>, 2014.
- Mankin, J. S., Viviroli, D., Singh, D., Hoekstra, A. Y., and Diffenbaugh, N. S.: The potential for snow to supply human water demand in the present and future, *Environmental Research Letters*, 10, 114 016, <https://doi.org/10.1088/1748-9326/10/11/114016>, 2015.
- Marsoner, T., Simion, H., Giombini, V., Egarter Vigl, L., and Candiago, S.: A detailed land use/land cover map for the European Alps macro region, *Scientific Data*, 10, 468, <https://doi.org/10.1038/s41597-023-02344-3>, 2023.
- 490 Marty, C., Michel, A., Jonas, T., Steijn, C., Muelchi, R., and Kotlarski, S.: SPASS – new gridded climatological snow datasets for Switzerland: Potential and limitations, <https://doi.org/10.5194/egusphere-2025-413>, 2025.
- Maussion, F., Butenko, A., Champollion, N., Dusch, M., Eis, J., Fourteau, K., Gregor, P., Jarosch, A. H., Landmann, J., Oesterle, F., Recinos, B., Rothenpieler, T., Vlug, A., Wild, C. T., and Marzeion, B.: The Open Global Glacier Model (OGGM) v1.1, *Geoscientific Model Development*, 12, 909–931, <https://doi.org/10.5194/gmd-12-909-2019>, 2019.
- 495 MeteoSwiss: Documentation of MeteoSwiss grid-data products: daily mean, minimum and maximum temperature: TabsD, TminD, TmaxD, Tech. rep., Federal Office of Meteorology and Climatology MeteoSwiss, Zurich, Switzerland, technical report, 2013.
- Molden, D., Sharma, E., Shrestha, A. B., Chettri, N., Pradhan, N. S., and Kotru, R.: Advancing Regional and Transboundary Cooperation in the Conflict-Prone Hindu Kush–Himalaya, *Mountain Research and Development*, 37, 502–508, <https://doi.org/10.1659/MRD-JOURNAL-D-17-00108.1>, 2017.
- 500 Nash, J. and Sutcliffe, J.: River flow forecasting through conceptual models part I — A discussion of principles, *Journal of Hydrology*, 10, 282–290, [https://doi.org/10.1016/0022-1694\(70\)90255-6](https://doi.org/10.1016/0022-1694(70)90255-6), 1970.



- O'Callaghan, J. F. and Mark, D. M.: The extraction of drainage networks from digital elevation data, *Computer Vision, Graphics, and Image Processing*, 27, 247, [https://doi.org/10.1016/S0734-189X\(84\)80047-X](https://doi.org/10.1016/S0734-189X(84)80047-X), 1984.
- Parajka, J. and Blöschl, G.: The value of MODIS snow cover data in validating and calibrating conceptual hydrologic models, *Journal of Hydrology*, 358, 240–258, <https://doi.org/10.1016/j.jhydrol.2008.06.006>, 2008.
- 505 Pesci, M. H., Schulte Overberg, P., Bosshard, T., and Förster, K.: From global glacier modeling to catchment hydrology: bridging the gap with the WaSiM-OGGM coupling scheme, *Frontiers in Water*, 5, 1296 344, <https://doi.org/10.3389/frwa.2023.1296344>, 2023.
- Quéno, L., Mott, R., Morin, P., Cluzet, B., Mazzotti, G., and Jonas, T.: Snow redistribution in an intermediate-complexity snow hydrology modelling framework, 18, 3533–3557, <https://doi.org/10.5194/tc-18-3533-2024>, 2024.
- 510 Reynolds, D. S., Pflug, J. M., and Lundquist, J. D.: Evaluating Wind Fields for Use in Basin-Scale Distributed Snow Models, *Water Resources Research*, 57, <https://doi.org/10.1029/2020WR028536>, 2021.
- RGI Consortium: Randolph Glacier Inventory - A Dataset of Global Glacier Outlines, Version 6, <https://doi.org/10.7265/4m1f-gd79>, [Indicate subset used]. Boulder, Colorado USA. NSIDC: National Snow and Ice Data Center, 2017.
- Rounce, D. R., Hock, R., Maussion, F., Hugonnet, R., Kochtitzky, W., Huss, M., Berthier, E., Brinkerhoff, D., Compagno, L., Copland, L., Farinotti, D., Menounos, B., and McNabb, R. W.: Global glacier change in the 21st century: Every increase in temperature matters, *Science*, 379, 78–83, <https://doi.org/10.1126/science.abo1324>, 2023.
- 515 Schulla, J. and Jasper, K.: Model Description WaSiM-ETH, Internal report, IAC, ETH Zurich, 2001.
- Stahl, K., Moore, R. D., Shea, J. M., Hutchinson, D., and Cannon, A. J.: Coupled modelling of glacier and streamflow response to future climate scenarios, 44, 2007WR005 956, <https://doi.org/10.1029/2007WR005956>, 2008.
- 520 Sturm, M., Goldstein, M. A., and Parr, C.: Water and life from snow: A trillion dollar science question, *Water Resources Research*, 53, 3534–3544, <https://doi.org/10.1002/2017WR020840>, 2017.
- Swisstopo - Swiss Federal Office of Topography: Swisstopo Digital Elevation Model (25m resolution), <https://www.swisstopo.admin.ch/en/geodata/height/alti3d.html>, accessed: 2024-06-21, 2020.
- Van Tiel, M. and Huss, M.: Daily cumulative glacier mass balances Swiss glaciers 1916–2023, ETH Zurich Research Collection [data set], <https://doi.org/10.3929/ethz-c-000786939>, 2025.
- 525 van Tiel, M., Kohn, I., Van Loon, A. F., and Stahl, K.: The compensating effect of glaciers: Characterizing the relation between interannual streamflow variability and glacier cover, *Hydrological Processes*, 34, 553–568, <https://doi.org/10.1002/hyp.13603>, 2020.
- van Tiel, M., Huss, M., Zappa, M., Jonas, T., and Farinotti, D.: Swiss glacier mass loss during the 2022 drought: persistent streamflow contributions amid declining melt water volumes, <https://doi.org/10.5194/egusphere-2025-404>, 2025.
- 530 Viviroli, D., Archer, D. R., Buytaert, W., Fowler, H. J., Greenwood, G. B., Hamlet, A. F., Huang, Y., Koboltschnig, G., Litaor, M. I., López-Moreno, J. I., Lorentz, S., Schädler, B., Schreier, H., Schwaiger, K., Vuille, M., and Woods, R.: Climate change and mountain water resources: overview and recommendations for research, management and policy, *Hydrology and Earth System Sciences*, 15, 471–504, <https://doi.org/10.5194/hess-15-471-2011>, 2011.
- Viviroli, D., Kumm, M., Meybeck, M., Kallio, M., and Wada, Y.: Increasing dependence of lowland populations on mountain water resources, *Nature Sustainability*, 3, 917–928, <https://doi.org/10.1038/s41893-020-0559-9>, 2020.
- 535 Von Der Esch, A., Huss, M., van Tiel, M., Berg, J., and Farinotti, D.: Modelling runoff in a glacierized catchment: the role of forcing product and spatial model resolution, <https://doi.org/10.5194/egusphere-2024-3965>, 2025.



- 540 Wang, L. and Liu, H.: An efficient method for identifying and filling surface depressions in digital elevation models for hydrologic analysis and modelling, *International Journal of Geographical Information Science*, 20, 193–213, <https://doi.org/10.1080/13658810500433453>, 2006.
- Wiersma, P., Aerts, J., Zekollari, H., Hrachowitz, M., Drost, N., Huss, M., Sutanudjaja, E. H., and Hut, R.: Coupling a global glacier model to a global hydrological model prevents underestimation of glacier runoff, *Hydrology and Earth System Sciences*, 26, 5971–5986, <https://doi.org/10.5194/hess-26-5971-2022>, 2022.
- 545 Winstral, A., Jonas, T., and Helbig, N.: Statistical downscaling of gridded wind speed data using local topography, *Journal of Hydrometeorology*, 18, <https://doi.org/10.1175/JHM-D-16-0054.1>, 2017.
- Zekollari, H., Huss, M., Schuster, L., Maussion, F., Rounce, D. R., Aguayo, R., Champollion, N., Compagno, L., Hugonnet, R., Marzeion, B., Mojtabavi, S., and Farinotti, D.: Twenty-first century global glacier evolution under CMIP6 scenarios and the role of glacier-specific observations, 18, 5045–5066, <https://doi.org/10.5194/tc-18-5045-2024>, 2024.